International Journal of Mechanical Engineering (IJME)
ISSN(P): 2319-2240; ISSN(E): 2319-2259
Vol. 5, Issue 6, Oct – Nov 2016; 11-24

International Academy of Science, Engineering and Technology
Connecting Researchers; Nurturing Innovations

EFFECT OF TEMPERATURE, STRAIN RATE AND COEFFICIENT OF FRICTION ON DEEP DRAWING PROCESS OF 6061 ALUMINUM ALLOY

CHENNAKESAVA R ALAVALA

Professor, Department of Mechanical Engineering, JNTUH College of Engineering, Hyderabad, India

ABSTRACT

Deep drawing is an essential process used for producing cups from sheet metal in large quantities. So, understanding the mechanics of the cup drawing process helps in determining the general parameters that affect the deep drawing process. There are generally two methods of analysis: experimental and numerical. Experimental analysis can be useful in analyzing the process to determine the process variables that produce a defect free product. However, experimental work is usually very expensive and time consuming to perform. On the other hand, the numerical modeling can be used to model and analyze the process through all stages of deformation. This paper deals with the analysis of deep drawing of circular blanks into axi-symmetric cylindrical cups forming using finite element analysis. The present work emphasizes the formability of cylindrical cups using high temperature-high strain rate (HTHSR) super plastic forming process. A statistical approach based on Taguchi Techniques and finite element analysis were adopted to determine the formability of 5656 Al alloy cups. The process parameters were temperature, strain rate, coefficient of friction and blank holder velocity. The FEA results obtained using finite element software namely D-FORM were validated through the experimental results. For 6061 Al alloy, the HTHSR super plastic forming process has happened at strain rate 0.1 s^{-1} and temperature of 300^{o}C.

KEYWORDS: 6061 Al Alloy, High Temperature, High Strain Rate, Super Plastic Deep Drawing Process, Coefficient of Friction, Cylindrical Cups, Forming Limit Diagram

INTRODUCTION

Deep drawing process is a noteworthy manufacturing process for producing large variety of automotive parts and aerospace parts as well as consumer products. Cup drawing, further its prominence as forming process, also helps as a basic test for the sheet metal formability. The process variables which involve in the success or failure of the cup drawing are the punch and die radii, the punch and die clearance, the press speed, the strain rate, the temperature and the coefficient of friction [1-5]. The blank holder force required to hold a blank flat for a cylindrical draw varies from very little to a maximum about one third of the drawing pressure [1].

The conventional super plastic forming is carried out at low strain rates in the range of 10-4 – 10-3 s -1 and high temperatures above recrystallization [6]. Several investigations have been carried out to boost the super plastic properties of aluminum alloys. Further, high temperature and high strain rate (HTHSR) super plastic forming process was developed to reduce the forming time of several aluminum alloys such as AA1050 [7], AA2014 [8], AA2017 [9], AA2024 [10], AA2219 [11], AA2618 [12], AA3003 [13], AA5049 [14] and AA5052 [15]. In the finite element simulations, a forming limit diagram (FLD) has been successfully applied to analyze the fracture phenomena by comparing the strain status [16].

AA6061 is a precipitation-hardened aluminum alloy, containing magnesium and silicon as its major alloying elements. The 6061 Al alloy is used in construction of aircraft structures, such as wings and fuselages, more commonly in homebuilt aircraft than commercial or military aircraft [17]. Other applications include: camera lens mounts, couplings, marines fittings, electrical fittings, hinge pins, magneto parts, brake pistons, hydraulic pistons, appliance fittings, valves and valve parts and bike frames. The significance of the present work was to determine suitability of 6061 aluminum alloy for high temperature and high strain rate super plastic forming process. The investigation was motivated on the process variables such as temperature, strain rate, coefficient of friction and blank holder velocity. The design of experiments was carried out using Taguchi technique and HTHSR super plastic deep drawing process was implemented using the finite element analysis software namely D-FORM 3D. The results acquired through the finite element analysis were endorsed experimentally.

MATERIALS AND METHODS

In the present work, 6061 Al alloy was used to fabricate cylindrical cups. The levels chosen for the controllable process parameters are summarized in table 1. The orthogonal array (OA), L9 was selected to carry out experimental and finite element analysis (FEA). The assignment of parameters in the OA matrix is given in table 2.

Table 1: Control Parameters and Levels

Factor	Symbol	Level–1	Level–2	Level–3
Temperature, ^{0}C	A	300	400	500
Strain rate, 1/s	B	0.1	0.5	1.0
Coefficient of friction	C	0.10	0.15	0.20
BH velocity, mm/s	D	0.13	0.`7	0.20

Table 2: Orthogonal Array (L9) and Control Parameters

Treat No.	A	B	C	D
1	1	1	1	1
2	1	2	2	2
3	1	3	3	3
4	2	1	2	3
5	2	2	3	1
6	2	3	1	2
7	3	1	3	2
8	3	2	1	3
9	3	3	2	1

Fabrication and Testing of Deep Drawn Cups

The sheets of 6061 Al alloy were cut to the required blank size. The blank specimens were heated in a muffle furnace to the desired temperature as per the design of experiments. The blank force was calculated using Eq. (1). The cups were fabricated using hydraulically operated deep drawing machine.

Drawing force, $F_d = \pi \mathrm{dt}\lceil D/d - 0.6 \rceil \sigma_y$ (1)

Clearance, $c = t \pm \mu\sqrt{10t}$ (2)

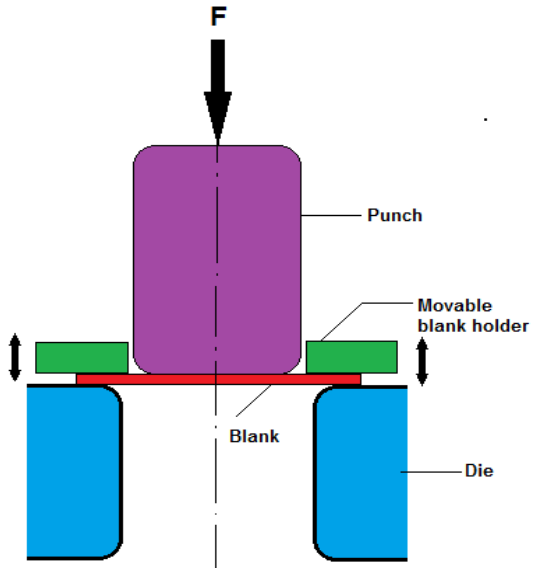

Figure 1: Deep Drawing Process with Movable Blank Holder

Finite Element Modeling and Analysis

The finite element modeling and analysis was carried using D-FORM 3D software. The cylindrical sheet blank was created with desired diameter and thickness using CAD tools. The cylindrical top punch, cylindrical bottom hollow die were also modeled with appropriate inner and outer radius and corner radius using CAD tools. The clearance between the punch and die was calculated as in Eq. (2).

In the present work, moving blank die was used to hold the blank at a predefined speed different to the punch speed. The contact between blank/punch and die/blank were coupled as contact pair (figure 1). The mechanical interaction between the contact surfaces was assumed to be frictional contact and modeled as Coulomb's friction model as defined in Eq. (3). The finite element analysis was chosen to find the metal flow, effective stress, height of the cup, and damage of the cup. The finite element analysis was carried out using D-FORM 3D software according to the design of experiments. The Coulomb's friction model was given by

$$\tau_f = \mu p \tag{3}$$

RESULTS AND DISCUSSIONS

The sheet blank was meshed with 14174 tetrahedral elements. The punch and blank holder are movable and non-deformable bodies. The bottom die is stationary and non-deformable body. The sheet blank is only deformable body in this work.

Influence of Process Parameters on Von Mises Stress

The percent contributions of A, B, C and D are, respectively, 38.55%, 37.17%, 17.86% and 6.42% towards variation in the von Mises stress (Table 3). Figure 2 presents the von Mises stress developed in 6061 Al alloy during cup drawing process as a function of temperature. It is observed that the von Mises stress increases with an increase in initial blank temperature from 300 to 400^{o}C and later on it decreases from 400 to 500^{o}C. As seen from figure 3, for trials 1, 2 and 3, the von Mises stress is lower than that of other trials. Also, for trials 4, 5 and 6 the von Mises stress is higher than that of remaining trials. Heating the sheet to 300^{o}C prior to deep drawing process is insufficient to recrystallize the 6061 Al alloy

into fine grain structure on subsequent cooling in air as shown in figure 2. Fine grain structure is attained in the 6061 Al alloy on heating to 400°C and later on cooling in air. However, the precipitates are formed at the grain boundaries when the 6061 Al alloy is heated to 500°C and successive cooling in air. The von Mises stress is the highest for the fine grain structure, the lowest for coarse grain structure and intermediate for precipitate grain structure.

Table 3: ANOVA Summary of the Von Mises Stress

Source	Sum 1	Sum 2	Sum 3	*SS*	*v*	*V*	*P*
A	1067.52	1014.77	827.05	10649.73	2	5324.87	38.55
B	1113.05	900.57	895.71	10267.41	2	5133.70	37.17
C	1052.08	976.78	880.48	4932.39	2	2466.20	17.86
D	1029.04	945.35	934.94	1773.97	2	886.98	6.42
e				0.00	0		0.00
T	4261.69	3837.48	3538.18	27623.50	8		100.00

Note: *SS* is the sum of square, *v* is the degrees of freedom, *V* is the variance, *F* is the Fisher's ratio, *P* is the percentage of contribution and *T* is the sum squares due to total variation.

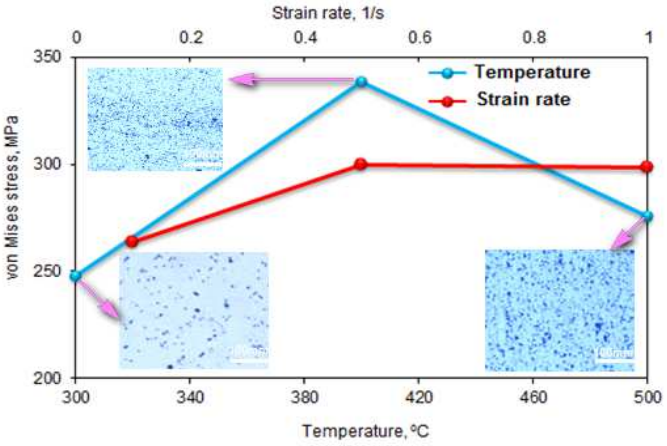

Figure 2: The Von Mises Stress as a Function of Temperature and Strain Rate

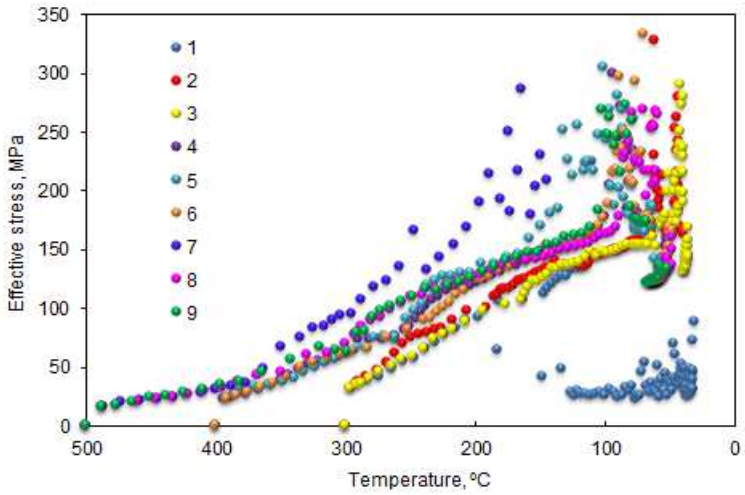

Figure 3: Effect of Temperature on Von Mises Stress for All Trials

The von Mises stress increases with increasing strain rate as shown in figure 2. Strain hardening is a result of plas-

tic deformation, a permanent change in shape to ensue cylindrical cup. An increase in the von Mises stress is effective for the change in the strain rate from 0.1 to 0.5 s-1and it is nearly continuous from 0.5 to 1.0 s-1 of strain rate. As seen from figure 4 the increasing gradient of von Misses stress is higher from 0.1 to 0.5 s^{-1} than that from 0.5 to 1.0 s^{-1} of strain rate.

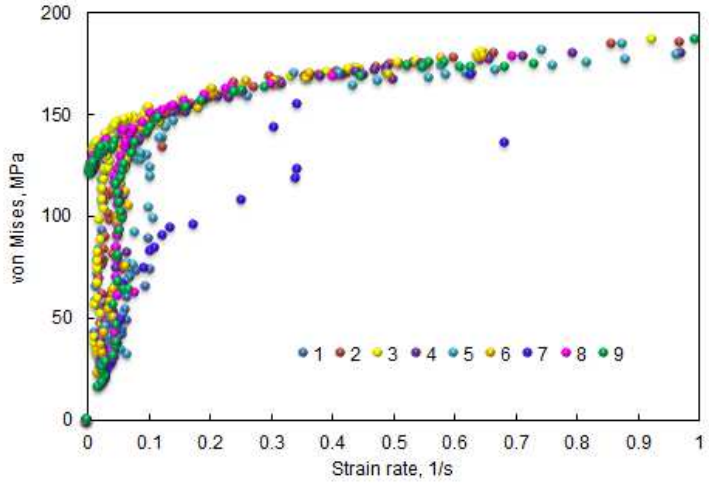

Figure 4: Effect of Strain Rate on Von Mises Stress for All Trials

Figure 5 depicts the von Mises stress as a function of COF (coefficient of friction) and blank holed (BH) velocity. It is observed that the von Mises stress increases with increase of COE and BH velocity, respectively, from 0.1 to 0.15 and 0.13 to 0.17 mm/s. In deep drawing process, friction initiates from sliding contact between the tool and the blank sheet. The surface asperities of the blank sheet undergo stretch deformation on account of the tangential load along the sliding contact. Once the surface asperities become flattened due to stretch deformation, further increase of friction does not demand large drawing force and consequently fall in the von Mises stress for the change of friction from 0.15 to 0.20. In the present work, the blank holder was allowed to move along with the punch but at different velocities to avoid wrinkles in the cup instead of applying different pressure values on the immovable blank holder [18, 19]. As the blank holding force was maintained constant in this work. The BH velocities were designed to avoid additional frictional force on the blank sheet and merely to avoid the formation of wrinkles in the flange area of the cup. The change in BH velocity from 0.17 to 0.20 does not bring any change in the von Mises stress.

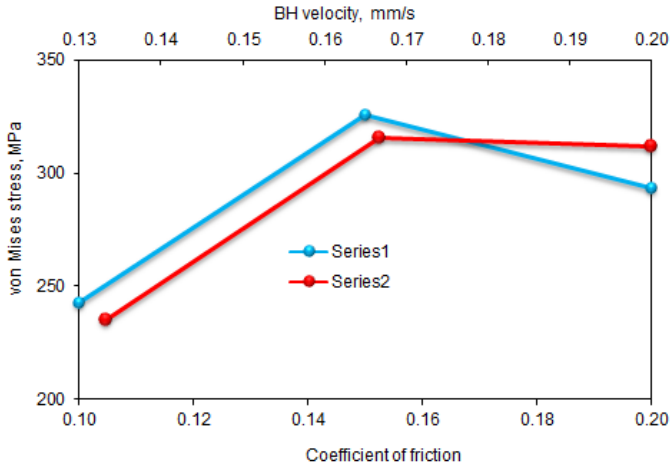

Figure 5: The Von Mises Stress as a Function of COF and BH Velocity

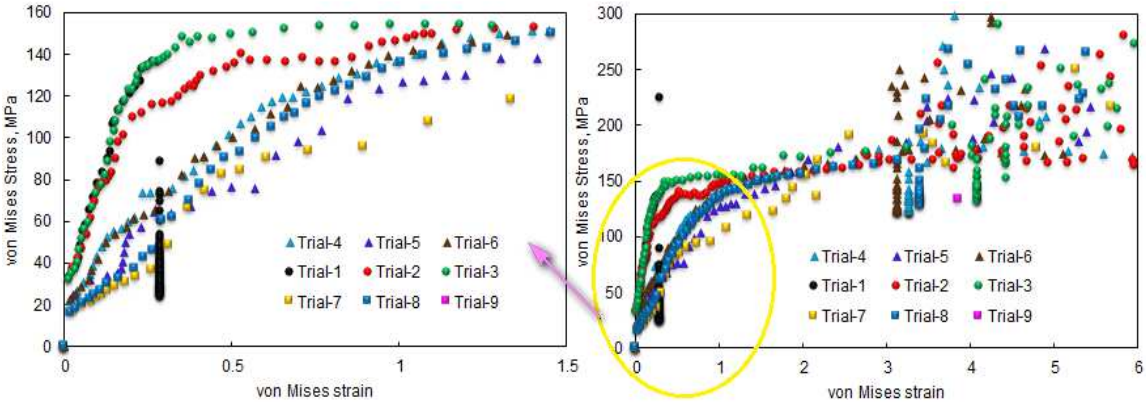

Figure 6: Effect of Process Parameters on the von Mises Stress (a) and True Stress-True Strain Curve of 6061 Al Alloy (b)

The FEA results of von Mises stress as a function of von Mises strain are shown in figure 6 for various test conditions as per the design of experiments. For trials 1, 2 and 3, the temperature was 300^{o}C and other process parameters were varied as mentioned in tables 1 and 2. The maximum values of von Mises stresses for trails 1, 2 and 3 are, respectively, 127, 327 and 290 MPa. AS observed from figures 2 and 5, the von Mises stress is low for level-1 values of process variables. Accordingly, the von Mises stress is 127 MPa as shown in figure 4. For trials 2 and 3, the process variables have values of level-2 and level-3, respectively, except temperature which is at 300^{o}C. The von Mises stresses for trails 2 and 3 are increased conferring to changes in the process variables. The slight decreased values are also observed for von Mises stress at level-3 of process variables as seen from figure 2 and 5. For trials 4, 5 and 6, the temperature was 400^{o}C and other process parameters were varied as mentioned in tables 1 and 2. The maximum values of von Mises stresses for trails 4, 5 and 6 are, respectively, 377, 305 and 333 MPa. These high values are due to fine grain structure in the sheet during deep drawing process. For trials 7, 8 and 9, the temperature was 500^{o}C and other process parameters were varied as mentioned in tables 1 and 2. The maximum values of von Mises stresses for trails 7, 8 and 9 are, respectively, 286, 268 and 273 MPa. The drop in stress values are on account of softening at 500^{o}C.

Influence of Process Parameters on Surface Expansion Ratio

In the deep drawing process the plastic deformation in the surface is much more prominent than in the thickness. As per the ANOVA summary of surface expansion ratio given in table 4., the temperature, (A), strain rate (B), coefficient of friction (C), and BH velocity (D) contribute, respectively, 13.05%, 23.88%, 42.47% and 16.96% respectively towards variation in the surface expansion ratio.

Table 4: ANOVA Summary of the Surface Expansion Ratio

Source	Sum 1	Sum 2	Sum 3	*SS*	*v*	*V*	*P*
A	66.74	41.43	19.46	373.18616	2	186.59308	13.05
B	45.62	72.9	9.11	682.92696	2	341.46348	23.88
C	6.25	89.56	31.82	1214.2543	2	607.12714	42.47
D	5.12	75.73	33.52	485.01069	2	242.50534	16.96
e				103.87	0		0
T	123.73	279.62	93.91	2859.25	8		100.00

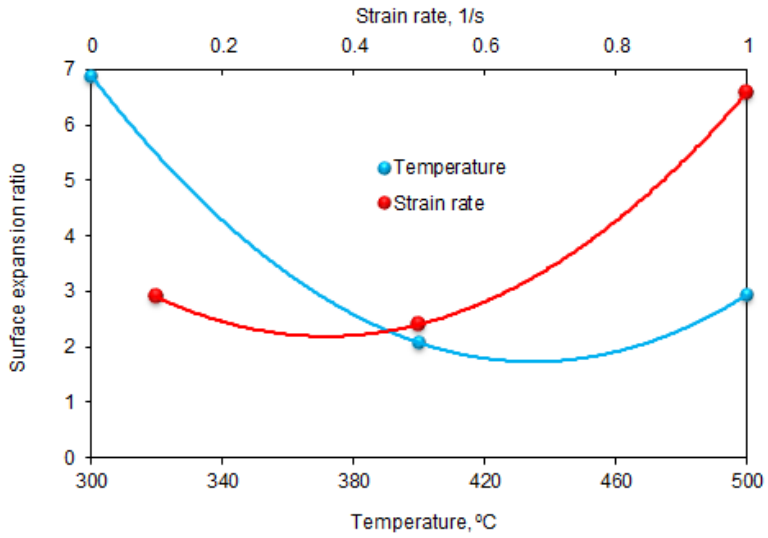

Figure 7: The Surface Expansion Ratio as a Function of Temperature and Strain Rate

The surface expansion ratio decreases with an increase in the operating blank temperature from 300^{o}C to 400^{o}C as shown in figure 7. For the operating temperature of 400^{o}C, the surface expansion ratio is consequence for fine recrystallization. The effect of strain rate on the surface expansion ratio is also shown in figure 7. The surface expansion ratio increases with an increase in the strain rate from 0.1 to 1.0 s^{-1}. The degree of recrystallization is dependent on thermo-mechanical processing conditions including temperature and strain rate of the sheet blank.

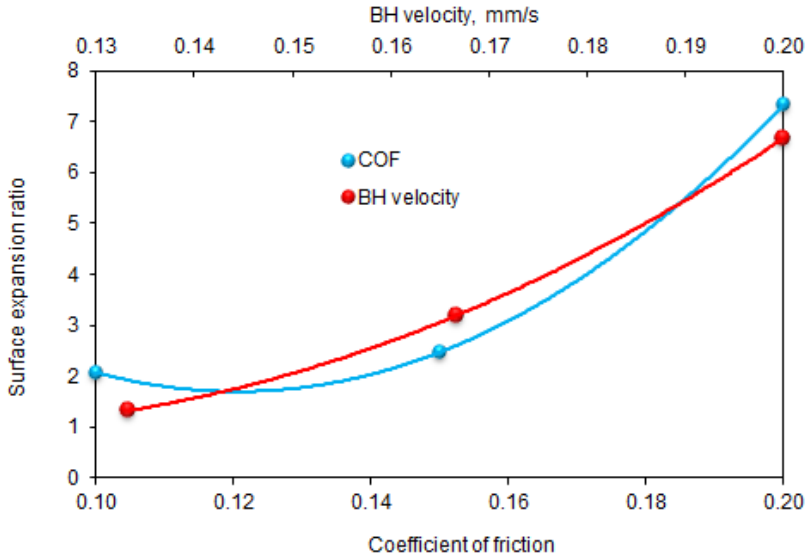

Figure 8: The Surface Expansion Ratio as a Function of COF and BH Velocity

The surface expansion ratio increases with increasing of COE as shown in figure 8. The surface expansion ratio is high for the COE of 0.20 due to stretch deformation as shown in figure 10. The surface expansion ratio was increased with an increase in the blank holder velocity from 0.13 to 0.20 mm/s as shown in figure 8. At high velocities, the blank holder comes in contact with the blank early and accordingly, the material is restrained to flow into the die resulting reduction in the surface expansion ratio. The FEA results of surface expansion ratio are revealed in figure9 for various test conditions as per the design of experiments. For the best quality of cup, the surface expansion ratio should be less than 2.0.

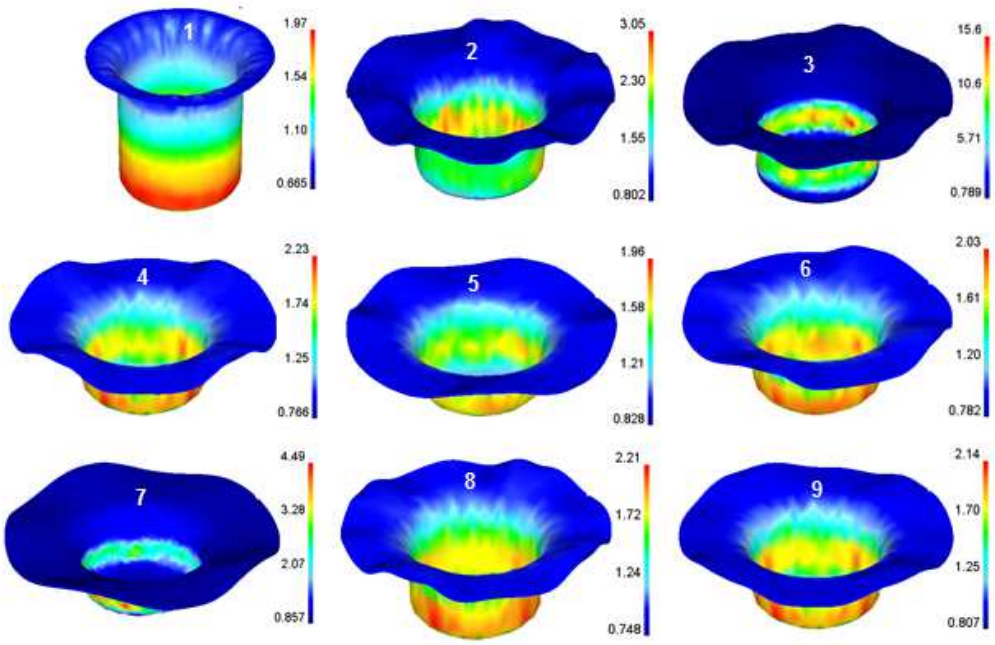

Figure 9: Effect of Process Parameters on the Surface Expansion Ratio

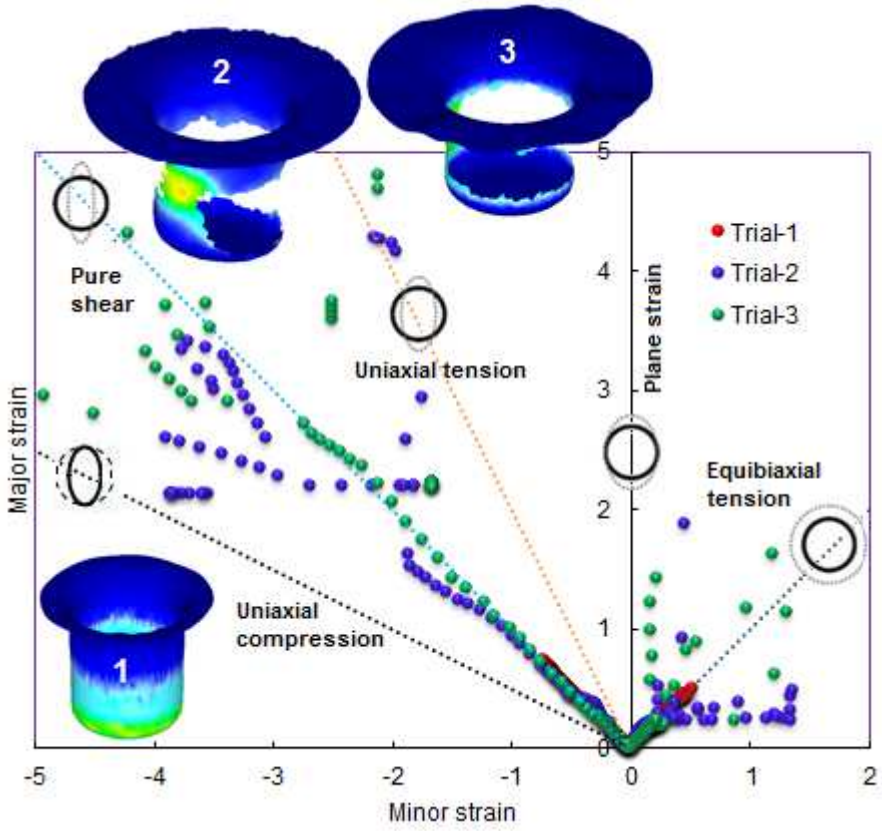

Figure 10: Forming Limit Diagram with Damage in the Cups Drawn at Temperature 300°C

Forming Limit Diagrams and Damages in the Cups

Figure 10 depicts the forming limit diagram (FLD) with damages in the conical cups drawn from 6061Al alloy sheets at temperature 300°C. The FLD for the conical cup drawn under trial 1 follows pure shear resulting good quality

cup. The FLD for the conical cup drawn under trial 2 and 3 experiences uniaxial and equibiaxial tensions. Figure 11 illustrates the forming limit diagram and damages in the cups drawn from 6061 Al alloy sheets with trials, 4, 5 and 6 at temperature 400°C. Cups drawn on trials 4 and 5 have damaged due to stretching. For trial 6, the cup has fracture due to uniaxial tension.

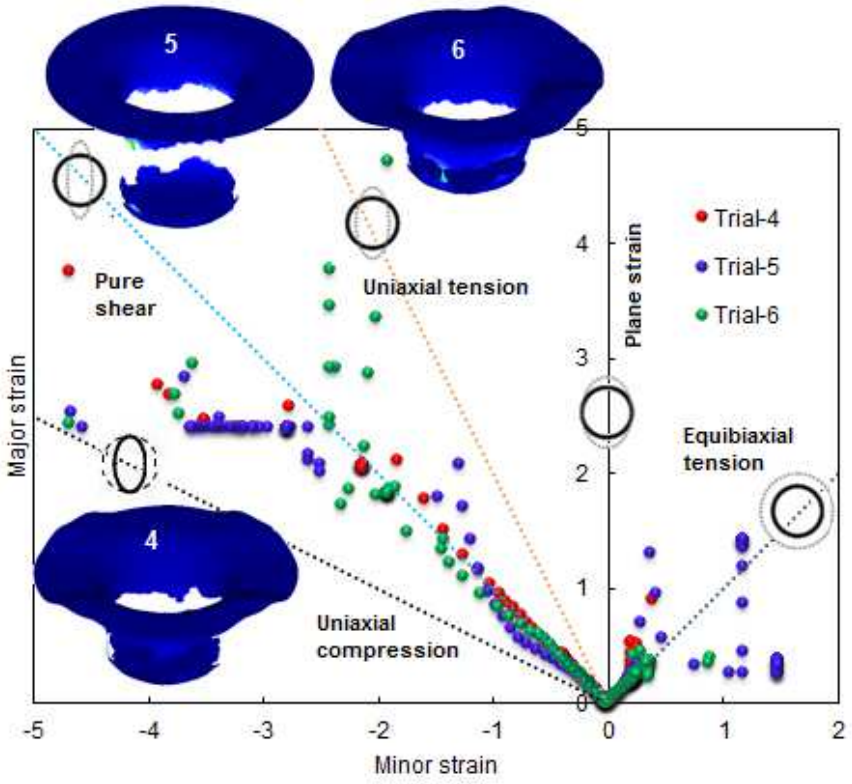

Figure 11: Forming Limit Diagram with Damage in the Cups Drawn at Temperature 400°C

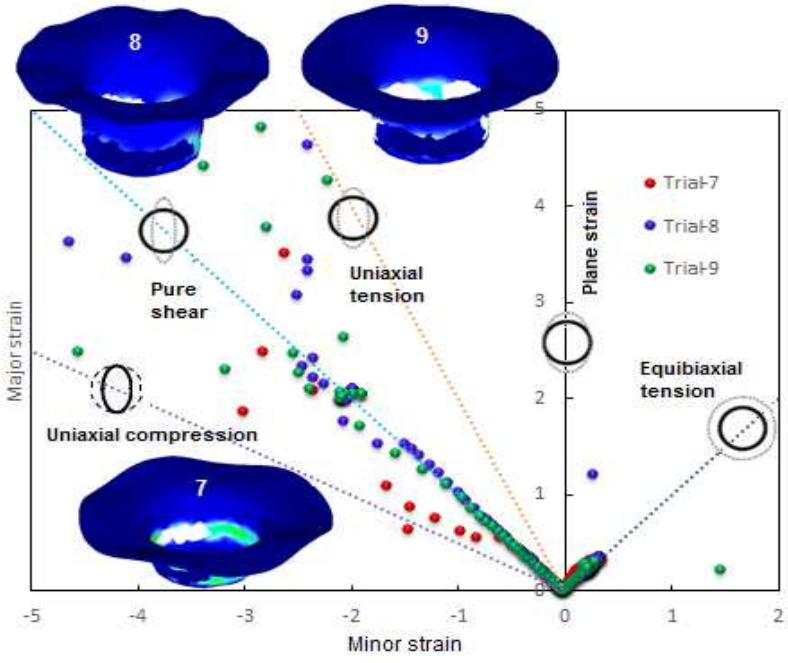

Figure 12: Forming Limit Diagram with Damage in the Cups Drawn at Temperature 500°C

Cups drawn from trials 7 and 9areraptured owing to uniaxial tension as shown in figure 12. Cup drawn with trial 8 conditions has failed due to uniaxial tension and stretching. As seen from figures 13 and 14 the shear stress induced in the cup drawn with trial 1 conditions is 47 MPa which is lower than those shear stress values induced in the rest of the cups. The maximum allowable shear stress for 6061 Al alloy is 36 MPa. The microstructure of cup drawn with trial 1 conditions reveals no fracture at grain boundaries as shown in figure 15a. The microstructure of cup drawn with trial 5 conditions reveals fracture at grain boundaries as shown in figure 15b. The microstructure of cup drawn with trial 9 conditions reveals cleavages at grain boundaries as shown in figure 15c.

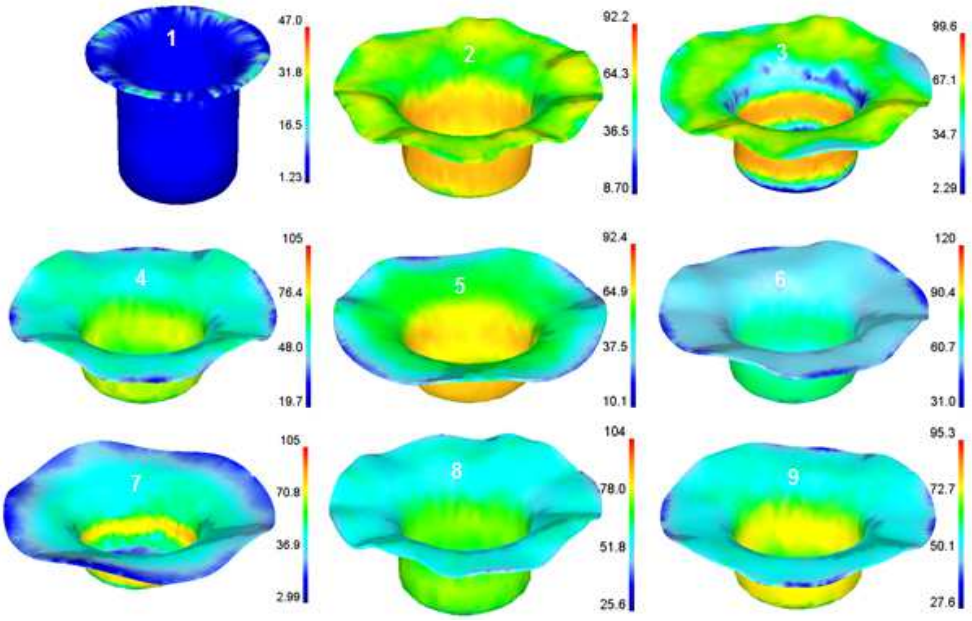

Figure 13: Shear Stress Induced in the Cups without Fracture

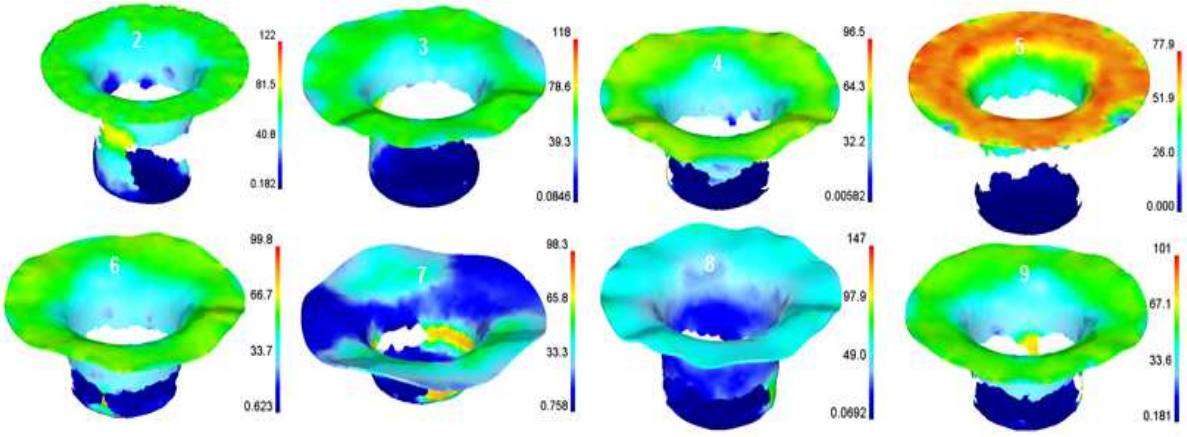

Figure 14: Shear Stress Induced in the Cups with Fracture

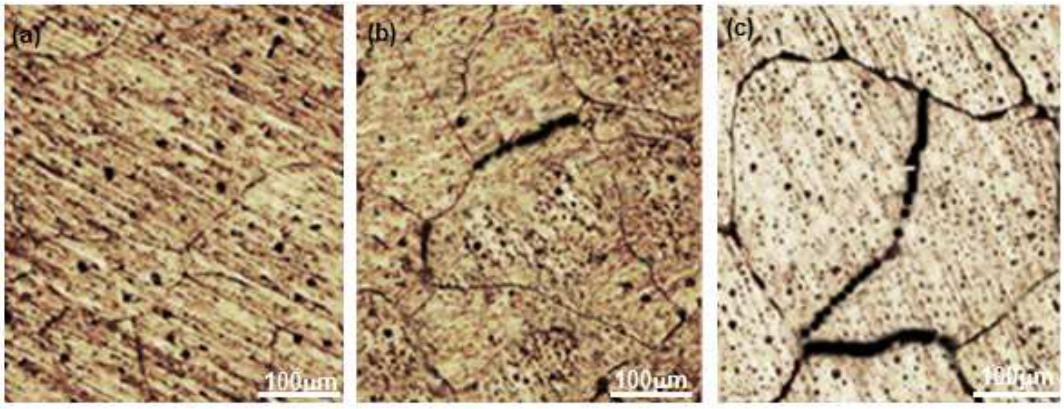

Figure 15: Microstrucutres of Drawn Cups (a) 300oC, (b) 400oC and (c) 500oC

In the present work, the critical value of the damage factor is defined as follows:

$$D_f = \int \frac{\sigma^*}{\sigma_{vm}} d\epsilon \tag{4}$$

where σ^* is the tensile maximum principal stress, σ_{vm} is the von Mises stress and $d\varepsilon$ is the effective strain increment. Fracture takes place when the damage factor has reached its critical value. The damage factors for all the trials are illustrated in figure 16. The least damage factor is associated with trail 1 of the design of experiments. Therefore, for the successful the optimum levels of the process variables are taken of trial 1 conditions of tables 1 and 2. Experimentally deep drawn cup with test conditions of trial 1 is shown in figure 17. The temperature and strain rate of trial 1 conditions are 300^{o}C and 0.1 s^{-1} which represent the high temperature and high strain rate superplastic forming process.

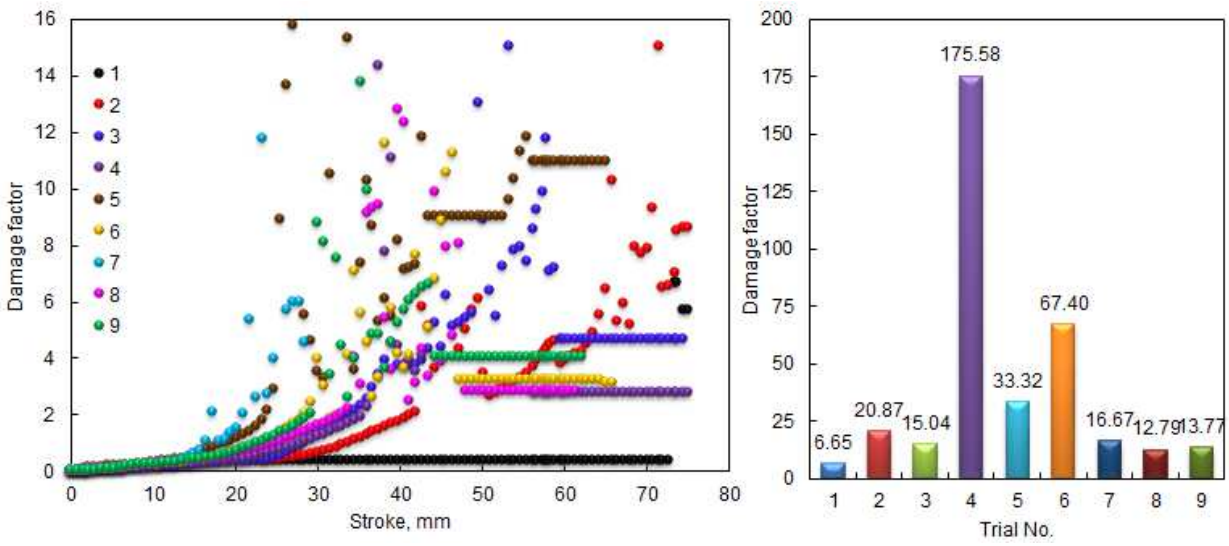

Figure 16: Damage Factors under Different Trials

Figure 17: Successful Cup Drawn with Trial 1 Conditions

CONCLUSIONS

In this process the draw ability of cylindrical cps from 6061 Al alloy has been demonstrated at high temperature and high strain rate conditions. The drawing stresses are increasing with increasing the temperature from 300 to 400^{o}C and strain rate from 0.1 to 0.5 s^{-1}, respectively. These effects are due to fine grain structure during the forming process. The wrinkling is reduced due to the movable blank holder.

REFERENCES

1. "Fundamentals of tool design," American Society of Tool and Manufacturing Engineers, New Delhi: Prentice Hall, 1983.
2. K. C. Park, Y. S. Kim,"The effect of material and process variables on the stamping formability of sheet materials," Journal of Material Processing Technology, Vol. 51, pp. 64−78, 1995.
3. A. C. Reddy, "Finite element analysis of reverse superplastic blow forming of Ti-Al-4V alloy for optimized control of thickness variation using ABAQUS," Journal of Manufacturing Engineering, Vol.1, pp.6-9, 2006.
4. A. C. Reddy, T. Kishen Kumar Reddy and M. Vidya Sagar, "Experimental characterization of warm deep drawing process for EDD steel," International Journal of Multidisciplinary Research & Advances in Engineering,Vol. 4, pp.53-62, 2012.
5. A. C. Reddy, "Evaluation of local thinning during cup drawing of gas cylinder steel using isotropic criteria," International Journal of Engineering and Materials Sciences, Vol. 5, pp. 71-76, 2012.
6. L.Carrino, G.Giuliano and S. Pistilli, "Numerical modelling of superplastic forming: some problems on the thinning evaluation," Transactions of NAMRI/SME XXIII, Vol. 23, pp. 51- 56, 1995.
7. A. C. Reddy, "Homogenization and Parametric Consequence of Warm Deep Drawing Process for 1050A Aluminum Alloy: Validation through FEA," International Journal of Science and Research, Vol. 4, pp. 2034-2042, 2015.
8. A. C. Reddy, "Parametric Optimization of Warm Deep Drawing Process of 2014T6 Aluminum Alloy Using FEA," International Journal of Scientific & Engineering Research, Vol. 6, pp. 1016-1024, 2015.
9. A. C. Reddy, "Finite Element Analysis of Warm Deep Drawing Process for 2017T4 Aluminum Alloy: Parametric Significance Using Taguchi Technique," International Journal of Advanced Research, Vol. 3, pp. 1247-1255,

2015.

10. A. C. Reddy, “Parametric Significance of Warm Drawing Process for 2024T4 Aluminum Alloy through FEA,” International Journal of Science and Research, Vol. 4, pp. 2345-2351, 2015.
11. A. C. Reddy, “Formability of High Temperature and High Strain Rate Superplastic Deep Drawing Process for AA2219 Cylindrical Cups,” International Journal of Advanced Research, Vol. 3, pp. 1016-1024, 2015.
12. A. C. Reddy, “High temperature and high strain rate superplastic deep drawing process for AA2618 alloy cylindrical cups,” International Journal of Scientific Engineering and Applied Science, Vol. 2, pp. 35-41, 2016.
13. A. C. Reddy, “Practicability of High Temperature and High Strain Rate Superplastic Deep Drawing Process for AA3003 Alloy Cylindrical Cups,” International Journal of Engineering Inventions, Vol. 5, pp. 16-23, 2016.
14. A. C. Reddy, “High temperature and high strain rate superplastic deep drawing process for AA5049 alloy cylindrical cups,” International Journal of Engineering Sciences & Research Technology, Vol. 5, pp. 261-268, 2016.
15. A. C. Reddy, “Suitability of High Temperature and High Strain Rate Superplastic Deep Drawing Process for AA5052 Alloy,” International Journal of Engineering and Advanced Research Technology, Vol. 2, pp. 11-14, 2016.
16. S. Kobayashi, S. I. Oh, T. Altan, “Metal forming and the finite method,” Oxford University Press, New York, 1989. pp. 23-35.
17. Aluminum Information at aircraftspruce.com, accessed October 13, 2006
18. Z. Q. Sheng, S. Jerathearanat, T. Altan,“Adaptive FEM simulation for prediction of variable blank holder force in conical cup drawing,” International Journal of Machine Tools andManufacturing, Vol. 44, pp. 487−494, 2004.
19. A. Wifi, A. Mosallam, “Some aspects of blank-holder force schemes in deep drawing process,” Journal of Achievements inMaterials and Manufacturing Engineering, Vol. 24,pp. 315−323, 2007.